***J. Ocean Univ. China*** (Oceanic and Coastal Sea Research)
DOI 10.1007/s11802-012-1897-7
ISSN 1672-5182, 2012 11 (3): 347-353
*http://www.ouc.edu.cn/xbywb/*
*E-mail:xbywb@ouc.edu.cn*

# Vertical Structure of the Tidal Currents on the Continental Shelf of the East China Sea

LI Lei[1)], JIANG Weiwei[2)], LI Peiliang[1), *], and YANG Bo[1)]

1) *Laboratory of Physical Oceanography*, *Ocean University of China*, *Qingdao* 266100, *P. R. China*
2) *National Marine Environmental Monitoring Center*, *Dalian* 116023, *P. R. China*

(Received October 13, 2011; revised November 23, 2011; accepted May 02, 2012)


**Abstract** The available data on tidal currents spanning periods greater than six months for the continental shelf of the East China Sea (26°30.052′N, 122°35.998′E) were analyzed using several methods. Tidal Current Harmonic Analysis results demonstrated that semi-diurnal tides dominated the current movement. The tidal currents of the principal diurnal and semidiurnal rotated clockwise with depth, with the deflection of the major semi-axes to the right in the upper layer and to the left in the lower layer. The vertical structures of two principal semi-diurnal constituents – $M_2$ and $S_2$ – were similar, which indicates that the tidal currents are mainly barotropic in this area. The main features of the variation of the four principal tidal constituents with depth demonstrate that the currents in this region are influenced by the upper and lower boundary layers. Therefore, the tidal constituents of the shallow water are similar. Different vertical modes were calculated based on the Empirical Orthogonal Function (EOF) analysis of the Eastern and Northern components of the tidal currents, with a variance contribution for the zero-order model of at least 90%. The variance contribution of the baroclinic model is minimal, which further reveals a strong barotropic character for the tidal currents of this region.

**Key words** continental shelf of the East China Sea; tidal current; vertical mode; barotropic tide

## 1 Introduction

Tidal currents are a manifestation of tidal movements, which are a prolonged and significant ocean phenomenon. The character and formation mechanisms of tidal movements are the focuses of physical oceanography in the east China seas. A number of studies on the tidal currents of the East China Sea have been performed since the mid-20th century (Sha, 2000; Chen *et al.*, 1995). A numerical simulation began in the 1980s on the tidal wave movement of the entire east China seas, including the Bohai Sea, Yellow Sea, and East China Sea (Wang *et al.*, 1999; Zhang *et al.*, 2005). Ding (1983) used observational data to analyze the tidal character and currents. Choi (1980), Zhao *et al*. (1994), and Ye and Mei (1995) simulated the tide of the East China Sea using a two-dimensional numerical model. The semi-diurnal tidal currents in the East China Sea were investigated by Shen and Ye (1984) on a three-dimensional scale to obtain the vertical variations in the tidal elliptical parameters. Fang (1986) thoroughly characterized the tides and tidal currents based on a combination of measurements and a series of highly accurate results from numerical modeling. Wan *et al*. (1998) simulated the movement of tide waves in the East China Sea on the continental slope using three-dimensional POM numerical modeling. These results have furthered our understanding of the tide waves in the East China Sea.

Almost all data from the East China Sea have been obtained in the offshore and northeastern regions, while long-term time series at the edge of the southeastern East China Sea continental shelf are very limited. Therefore, the character of the tidal currents in this area is not well understood. Data over a time period greater than six months were obtained by us using a mooring system deployed on the seabed of the East China Sea. The tidal constitutes and vertical structures are discussed in this paper.

The paper is organized as follows: the character of current data analyzed is described in Section 1; the mean flow is shown in Section 2; the results from the tidal harmonic analysis method used are analyzed in Section 3; the results from the Fast Fourier Transform method used are analyzed in Section 4; and the Empirical Orthogonal Function method used to obtain the vertical modes of the tidal currents is described in Section 5. Summary and conclusions are discussed in Section 6.

## 2 Data

The current data were obtained by an 300 kHz ADCP mounted on a mooring system on the seabed. The system

* Corresponding author. Tel: 0086-532-66782850
E-mail: lpliang@ouc.edu.cn

was located approximately 113 m deep at the edge of the East China Sea continental shelf (26˚30.052´N, 122˚35.998´E, see Fig.1). Measurements began at 21:20, September 19, 2008 and ended at 17:00, April 4, 2009 (Beijing time). The temporal resolution for the observation was 10 min and the vertical spacing was 8 m, there being a total of 13 layers. However, only 11 time series were successive and could be analyzed in this study. The depth of the layer closest to the surface and that of the deepest layer were 24 m and 104 m, respectively. The gaps in the time series, caused by instrumentation or weather, were estimated from adjacent measurements before further analysis.

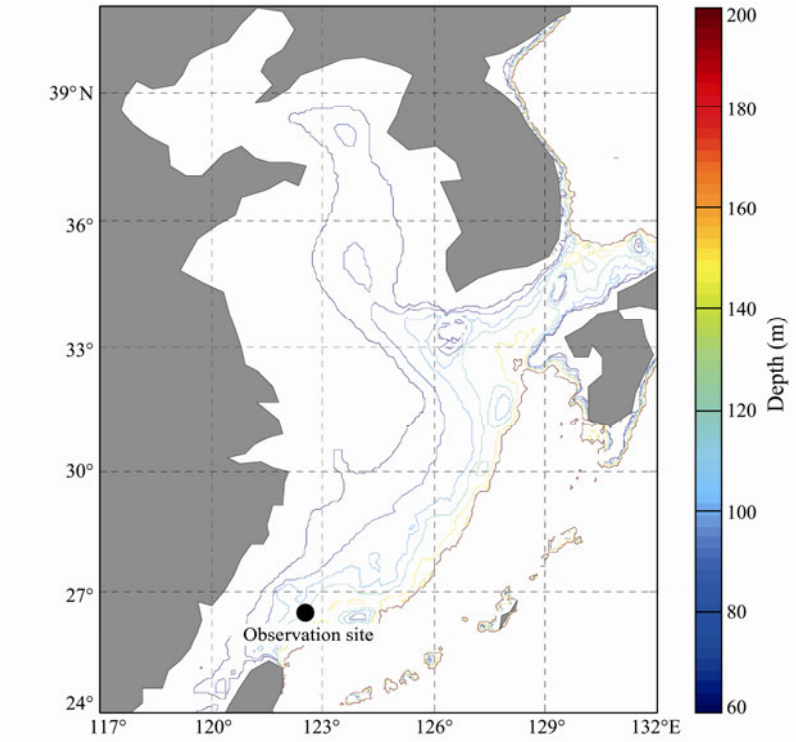


Fig.1 Bathymetric map of the Bohai Sea, Yellow Sea, and East China Seas. The black point indicates the observation site.

## 3 Mean Flow

The time-averaged current profiles (Fig.2) demonstrated that the eastern component (*U*) changes with depth more rapidly than the northern component (*V*). In general, the time-averaged current flowed in the northeastern direction. The current velocity reached a maximum at a depth within 40–50 m with the direction first turning right and then left.

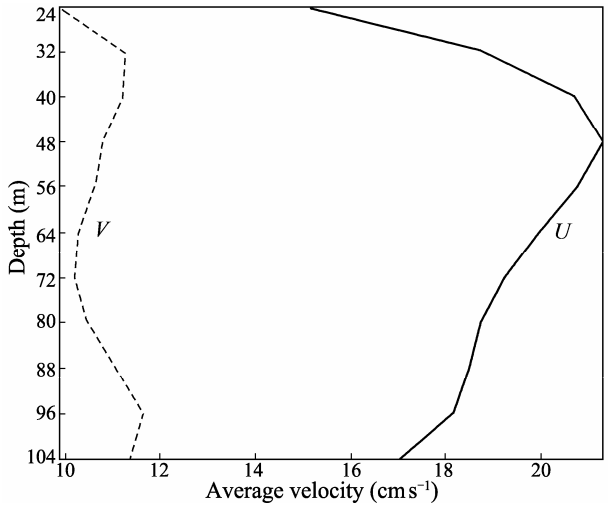


Fig.2 Profiles of time-averaged *U* and *V* components of observed currents. The solid line indicates the *U* component and the dashed line the *V* component. Positive *U* component indicates the current flowing in the east direction. Positive *V* component indicates the current flowing in the north direction.

## 4 Harmonic Analysis of Tidal Currents

By using the tidal harmonic analysis method, the harmonic constants of the tidal currents and elliptical parameters were calculated according to the frequencies. In this study, the Matlab software package provided by Pawlowicz *et al*. (2002) was used to calculate the harmonic constants and elliptical parameters for each observed tidal current series. The elliptical parameters consist of major and minor semi-axes (positive and negative values indicate anticlockwise and clockwise rotations of tidal currents, respectively), the inclination angles, and the Greenwich phases.

These results demonstrated that there are four principal tidal constituents, including two semidiurnal ($M_2$ and $S_2$) and two diurnal tidal constituents ($K_1$ and $O_1$). The semidiurnal tidal constituents are remarkable in this region, with $M_2$ as the most evident and $S_2$ as the second most evident component of these constituents. The ratios of the sum of the $K_1$ and $O_1$ major semi-axes to the sum of the

$M_2$ and $S_2$ major semi-axes are less than 0.5 in all layers (from surface to bottom, 0.17, 0.17, 0.17, 0.16, 0.15, 0.13, 0.11, 0.09, 0.08, 0.08, and 0.08, respectively), suggesting that the semi-diurnal tidal current is dominant in this area. The minor semi-axes of the four principal tidal constituents are given in Table 1. The sign of the minor axis indicates the direction of rotation, with positive and negative values representing counterclockwise and clockwise rotation, respectively. The minor semi-axes of the semidiurnal tidal constituents were negative in all observation layers, except for $S_2$ at 104 m, which indicated that the semidiurnal tidal ellipses veer gradually clockwise with depth. The diurnal tidal constituent, $K_1$, veers clockwise with depth up to 80 m, and then veers counterclockwise with depth greater than 80 m. The diurnal tidal constituent, $O_1$, veers clockwise with depth up to 72 m, and then veers counterclockwise with depth greater than 72 m.

Table 1 The minor semi-axes of the four principle tidal constituents (cm s$^{-1}$)

| Depth (m) | $M_2$ | $S_2$ | $K_1$ | $O_1$ |
|---|---|---|---|---|
| 24 | −5.693 | −1.972 | −3.045 | −1.231 |
| 32 | −5.036 | −1.83 | −2.864 | −1.006 |
| 40 | −4.39 | −1.827 | −2.821 | −1.03 |
| 48 | −3.949 | −1.915 | −2.441 | −0.95 |
| 56 | −3.784 | −1.893 | −1.748 | −0.679 |
| 64 | −4.06 | −1.67 | −0.964 | −0.372 |
| 72 | −4.449 | −1.888 | −0.117 | 0.318 |
| 80 | −4.69 | −1.785 | 0.392 | 0.989 |
| 88 | −4.198 | −1.219 | 0.863 | 1.263 |
| 96 | −3.123 | −0.468 | 1.118 | 1.323 |
| 104 | −1.733 | 0.034 | 1.042 | 1.042 |

The variations in major semi-axis and inclination angle for the four principal tidal constituents with depth are shown in Figs.3–4. All major semi-axes of $M_2$, $S_2$, and $K_1$ became greater and then gradually decreased with depth approximately. Remarkably, the major semi-axis of the tidal constituent $M_2$ remained steady with depth (Fig.3a). The maximum value was 41.14 cm s$^{-1}$ at 88 m, and the minimum value was 33.9 cm s$^{-1}$ at the bottom (104 m). The value varied around 40 cm s$^{-1}$. The inclination angle turned right slightly (from 139.36°to 140.12°) up to 32 m, then there was a minor oscillation of approximately 140° up to 72 m, and finally the angle rotated left at depths greater than 72 m. The variations in major semi-axis and inclination angle of the tidal constituent $S_2$ with depth are shown in Fig.3b, which is similar to the case with the $M_2$ constituent. The major semi-axis for $S_2$ also varied slightly with a maximum value of 15.57 cm s$^{-1}$ at 80 m and a minimum value of 11.93 cm s$^{-1}$ at the bottom (104 m). The value varied around 15.0 cm s$^{-1}$. The inclination angle turned right slightly from 134.77° to 135.48° up to 32 m, then oscillated around 135° up to 64 m, and turned left at depths greater than 64 m. The maximum amplitude for tidal constituent $K_1$ was at 32 m (Fig.4a), and the major semi-axis was 6.02 cm s$^{-1}$ at this depth. The amplitude decreased with depth and was reduced to 2.36 cm s$^{-1}$ at the bottom. The inclination angle of the tidal constituent $K_1$ varied around 135° at depths greater than 56 m and turned left from 56 m to 96 m (the inclination angle was 139.3° at 56 m and 91.6° at 96 m), with slight variations from 96 m to 104 m. The major semi-axis of the tidal constituent $O_1$ decreased with depth (Fig.4b) and most significantly at 24 m, the major semi-axis being 3.66 cm s$^{-1}$ at this depth. The major semi-axis was insignificant at other depths and was reduced to 1.37 cm s$^{-1}$ at the bottom (104 m). The inclination angle rotated from 122.7° at 24 m to 135.6° at 56 m and then to 150.2° with a right rotation at depths greater than 72 m, which was 118.1° at 88 m.

The variation of the four principal tidal constituents with depth demonstrates that the currents in this region are influenced by floor-friction, which is representative of the tidal constituents at shallower depths. These data also agree with the deflection of the major semi-axes direction to the

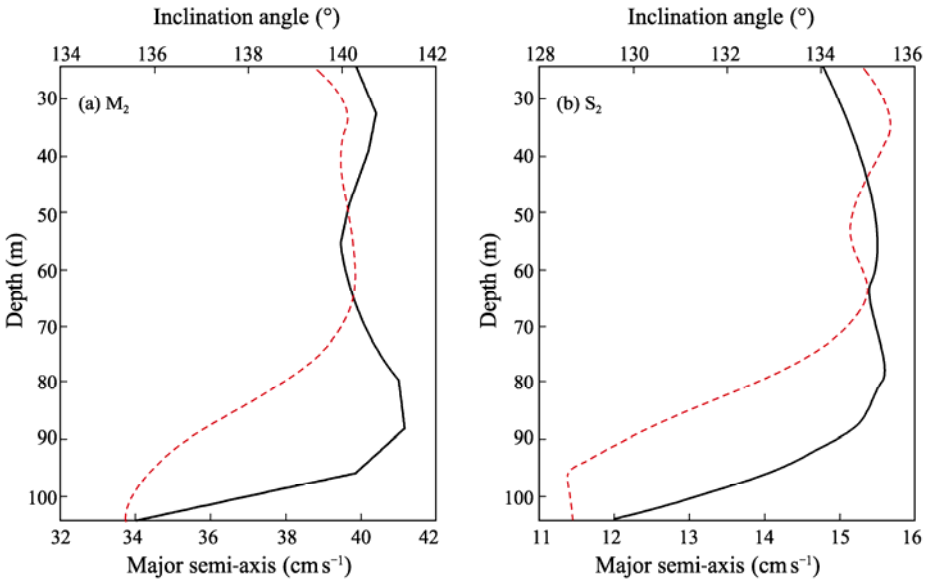


Fig.3 Major semi-axes and inclination angles of two semi-diurnal constituents varying with depth. The black line indicates the major semi-axis, and the dashed red line indicates the inclination angle: (a) Semi-diurnal constituent $M_2$, and (b) Semi-diurnal constituent $S_2$.

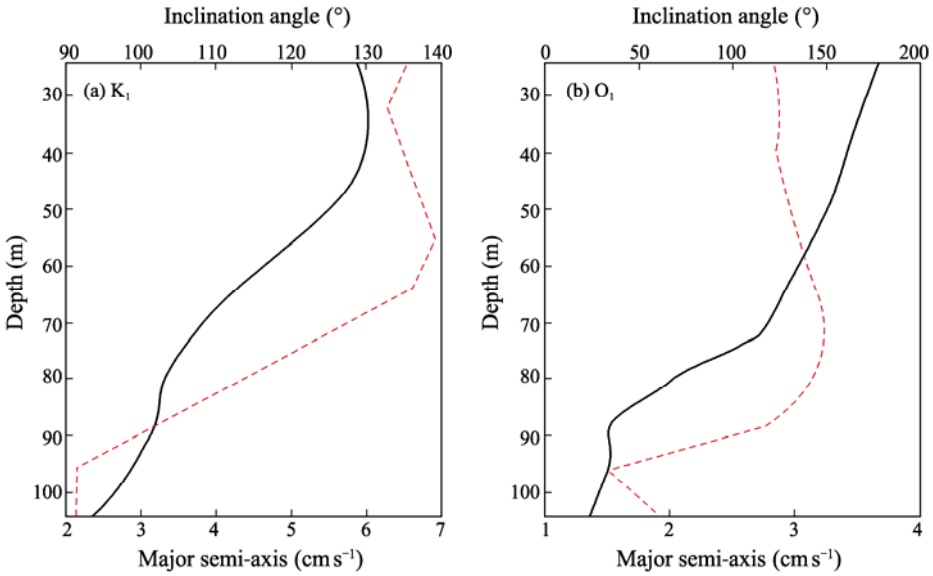


Fig.4 Major semi-axes and inclination angles of two diurnal constituents varying with depth. The thick black line indicates the major semi-axis, and the dashed red line indicates the inclination angle. (a) Diurnal constituent $K_1$, and (b) diurnal constituent $O_1$.

right or left at depths greater than 50m on the continental shelf (Ye, 1984). The $S_2$ elliptical parameters are similar to those of the $M_2$ constituent at all depths, indicating that the currents in this region are strongly barotropic.

## 5 Fast Fourier Transform (FFT)

Measurements at 32, 60, 80 and 104 m during the first four days were analyzed using the FFT method to explore the low frequency components of the observed currents (Note: the results can be obtained from any four consecutive days during the observation period) (Figs.5–8).

The FFT results reveal that the semidiurnal and diurnal constituents are dominant among the low frequency (less than 4cycle d$^{-1}$) constituents of the *U* and *V* components. However, the residual current constitutes a relatively large proportion of each time series, which suggests that there was a steady strong northeast current during the measured time period.

The ratios of the diurnal constituents to the semidiurnal constituents for the *U* and *V* components are different. The amplitude of the *V* component for the diurnal constituents is larger than the *U* component except for the time series at 64 m, suggesting that this current is more significant in the north-south direction. However, the amplitude of the *V* component for the semidiurnal constituents is smaller than that of the *U* component at all depths, which suggests that this current is more significant in the east-west direction. When the ratio of the diurnal constituents amplitude to the semidiurnal constituents amplitude is smaller than 0.5, the tidal currents have a half-day period, which suggests that the flow field is characterized by semidiurnal tidal currents. Teague *et al*. (1998) noted that the amplitude of the tidal current is depth-independ-

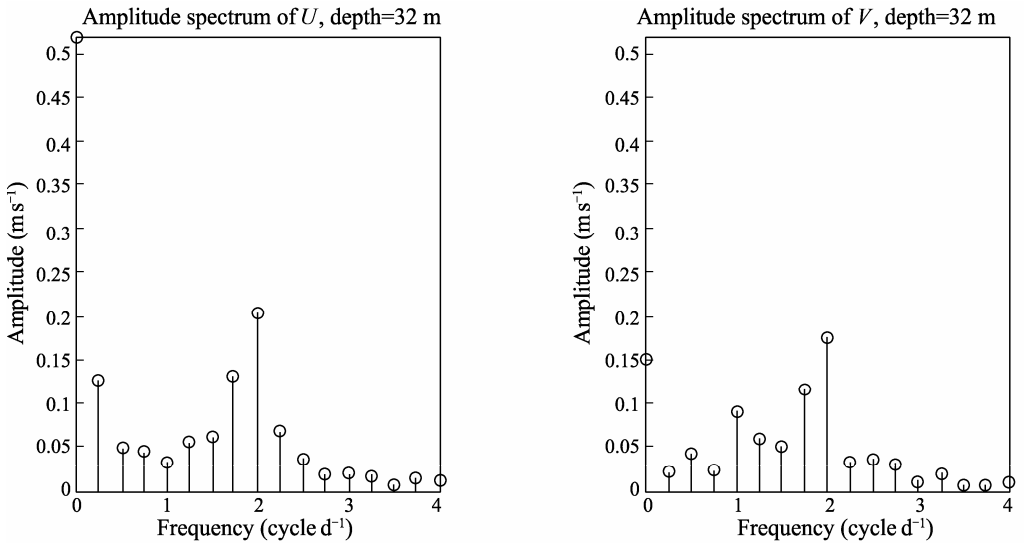


Fig.5 Amplitude spectra at 32 m. The left picture indicates the first 17 low frequency components of the *U* spectrum, and the right picture indicates the first 17 low frequency components of the *V* spectrum.

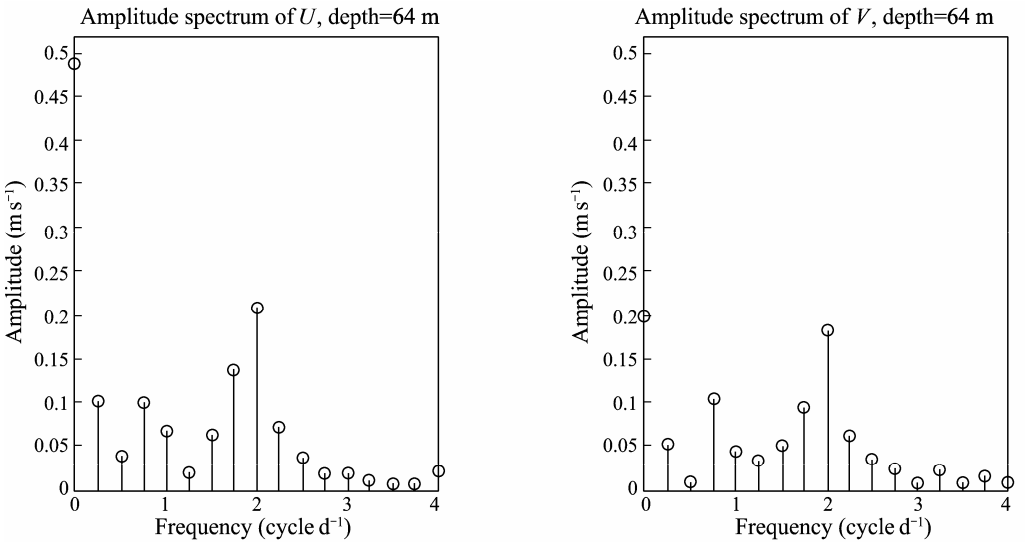


Fig.6 Amplitude spectra at 64 m. The left picture indicates the first 17 low frequency components of the *U* spectrum, and the right picture indicates the first 17 low frequency components of the *V* spectrum.

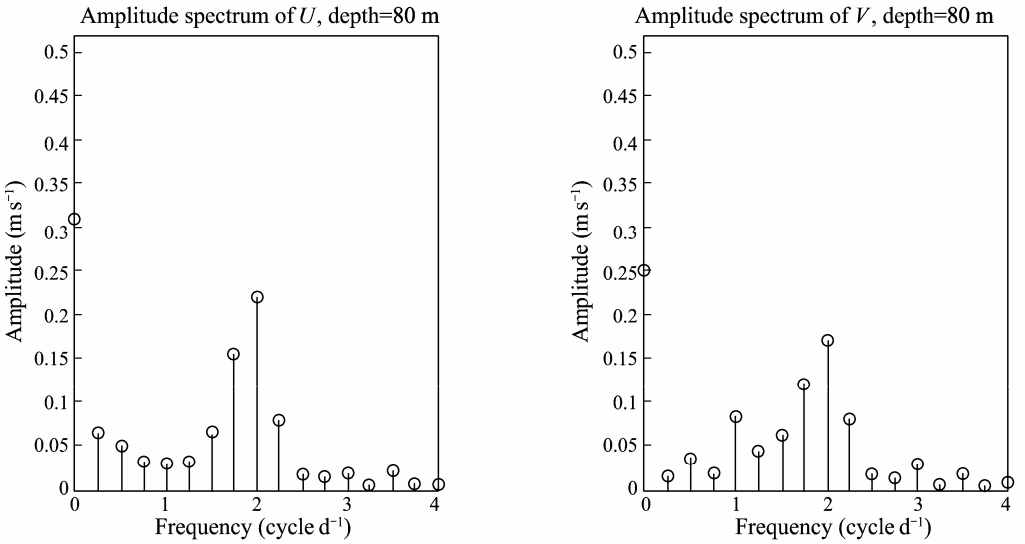


Fig.7 Amplitude spectra at 80 m. The left picture indicates the first 17 low frequency components of the *U* spectrum, and the right picture indicates the first 17 low frequency components of the the *V* spectrum.

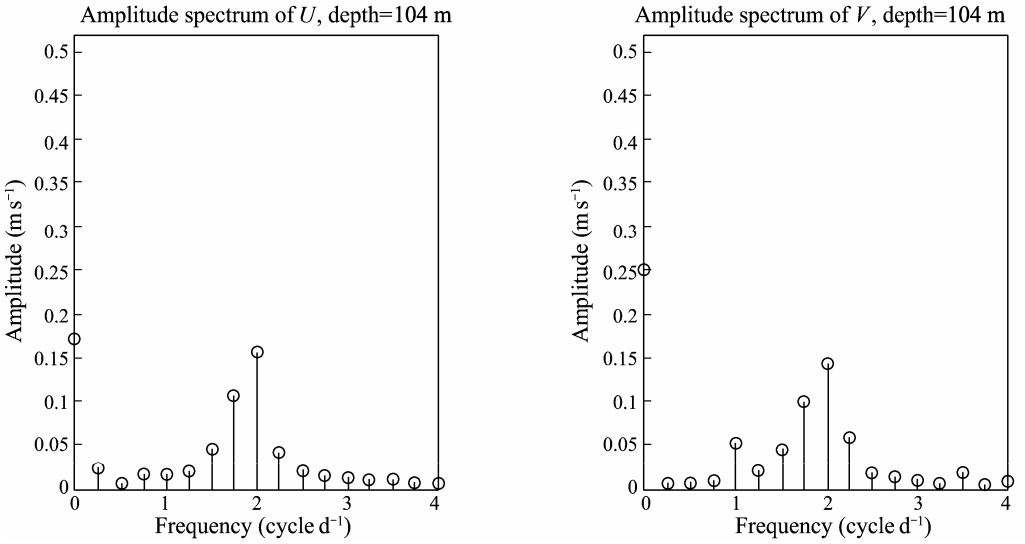


Fig.8 Amplitude spectra at 104 m. The left picture indicates the first 17 low frequency components of the *U* spectrum, and the right picture indicates the first 17 low frequency components of the the *V* spectrum.

ent for a barotropic tide. The observed amplitudes of the semi-diurnal tidal currents were almost uniform throughout the entire water column, indicating that there are strong barotropic currents in this region. These data are corroborated by the harmonic analysis results.

## 6 Vertical Modes of Tidal Currents

The Empirical Orthogonal Function (EOF) method is a kind of multivariate analysis that is used to investigate large amounts of data with temporal and spatial variations. The observed phenomenon is disassembled into spatial modes representing the spatial characteristics and temporal modes representing the temporal characteristics. These modes reveal the basic characteristics and evolution of the observed phenomena (Lagerloef and Berstein, 1988).

In our study $U$ and $V$ components were each analyzed with the EOF method to derive the typical spatial distribution field and the corresponding temporal coefficient. The first five EOF modes account for 99.42% of the variability in the $U$ component, with each respective mode accounting for 88.33%, 7.90%, 1.96%, 0.80%, and 0.43% of the variability. The first five modes of the $V$ component account for 99.1% of the variability, with each respective mode accounting for 84.61%, 10.03%, 2.61%, 1.22%, and 0.64% of the variability. The first five modes of the $U$ and $V$ components were at least 95% in the significance test.

Fig.9a shows the first five vertical modes of the $U$ component. The amplitudes indicate that the first mode is dominant with a variance contribution that is much larger than that in the other modes. The vertical modal amplitudes are all positive and the changes are small from top to bottom. The second mode reveals a reversed flow with direction changing at depth 58 m and is thus a first-order mode. For the third mode, the sign changes twice at 40.5 m and 78 m, and therefore is a second-order mode. The fourth and fifth modes are higher order modes. These four high-order modes account for about 11.1% of the variability.

Fig.9b shows the first five vertical modes of the $V$ component. The modes are in accordance with the $U$ components to a certain extent. The variation in the amplitude of the first mode with depth is similar to the $U$ component. The first mode is also the dominant one. The second mode reveals a reversed flow with the direction changing at depth 62.3 m, and therefore is a first-order mode. For the third mode, the sign changes twice at 41.7 m and 81.3 m, and it is thus a second-order mode. The fourth and fifth modes are higher order modes. These four high-order modes account for about 14.5% of the variability.

The first mode is the zero-order model that indicates the barotropic character of the current. The higher order modes characterizing the baroclinic tidal currents are relatively small. The time series of the first mode of $U$ and $V$ components has an obvious 12-hour period indicating the frequency composition of the barotropic current. These data agree with the harmonic analysis results, demonstrating that the flow has obvious barotropic features, which is primarily due to the significantly mixed water column in the winter associated with the strong sea surface wind and low SST.

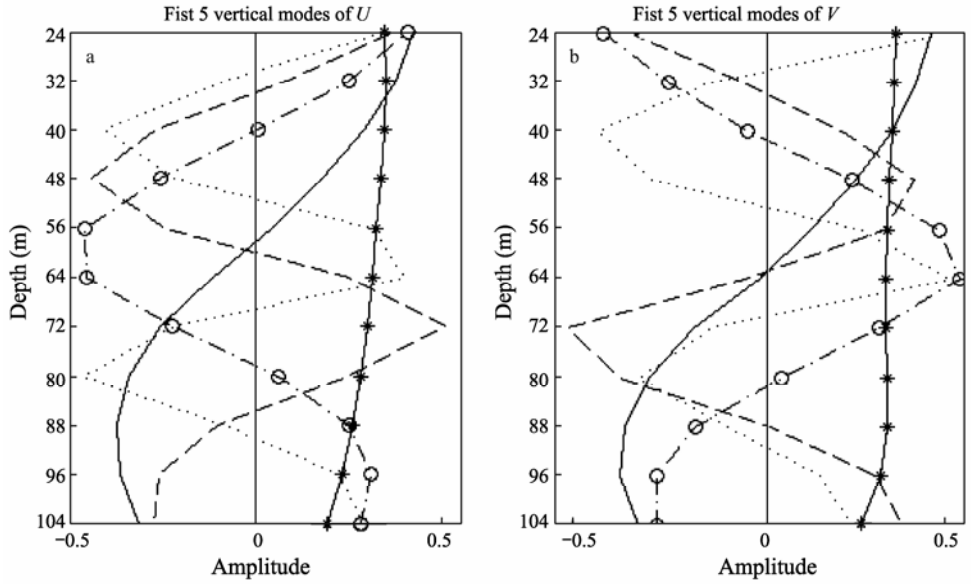


Fig.9 First 5 vertical modes varying with depth. '−∗' line indicates first mode; '−' line indicates second mode; '−·o' line indicates third mode; '−−' line indicates fourth mode; '··' line indicates fifth mode. a) $U$'s 5 modes, and b) $V$'s 5 modes.

## 7 Conclusions

The station where data were collected for this analysis is at the edge of the continental shelf in the East China Sea. Tidal current harmonic analysis, the fast Fourier transform, and the empirical orthogonal function were used to analyze the current data obtained over a period of more than six months. The results are as follows:

1) The harmonic analysis results show that the semidiurnal tidal constituents are remarkable in this region, with $M_2$ being the most significant and $S_2$ being the second

most significant of these tidal constituents. $K_1$ and $O_1$ are much smaller than the semidiurnal constituents. The ratio of the semidiurnal major semi-axis to the diurnal major semi-axis is less than 0.5 at all depths, which suggests that the normal semi-diurnal tides are dominant in this area.

2) The elliptical parameters of the semidiurnal tidal constituents $M_2$ and $S_2$ vary little with depth. The $S_2$ constituent is similar to the $M_2$ constituent at all measured depths, which indicates that the current of this region has a strong barotropic feature. The vertical modes of the *U* and *V* components are similar to those determined by using the EOF method. The variance contribution of the zero-order mode is much larger, and the time series involved has an obvious 12-hour period. These results indicate that the semidiurnal constituents are dominant in this area and that there is an obvious barotropic character of the tidal current. The barotropic character is associated with the shallow depth and strong convection.

3) The main features of the variation of the four principal tidal constituents with depth demonstrate that the current in this region is influenced by the upper and lower boundary layers. Therefore, the tidal constituents of the shallow water are similar.

4) The ellipses of the principal tidal constituents rotate clockwise with depth, with the deflection of the major semi-axes to the right in the upper layer and to the left in the lower layer.

## Acknowledgement

This work was supported by the National Basic Research Program of China (2007CB411807) and the National Natural Science Foundation of China (40806072, 41176009).

## References

Chen, Z. Y., Ye, A. L., and Zuo, J. C., 1995. Advances in ocean tide research over the past 40 years in China. *Journal of Ocean University of Qingdao*, **25** (4): 435-444.

Choi, B. H., 1980. *A Tidal Model of the Yellow Sea and the Eastern China Sea*. Korea Ocean Research and Development Institute, Korea, 72pp.

Ding, W. L., 1983. A study on the characteristics of tide and tidal current in the East China Sea. *Studia Marina Sinica*, **2** (1): 135-148.

Fang, G. H., 1986. Tide and tidal current charts for the marginal seas adjacent to China. *Chinese Journal of Oceanology and Limnology*, **4** (1): 1-16.

Lagerloef, G. S. E., and Berstein, R. L., 1988. Empirical orthogonal function analysis of advanced very high resolution radiometer sea surface temperature patterns in Santa Barbara Channel. *Journal of Geophysical Research*, **93** (C6): 6863-6873.

Pawlowicz, R., Beardsley, B., and Lentz, S., 2002. Classical tide harmonic analysis including error estimates in MATLAB using T_TIDE. *Computers and Geosciences*, **28**: 929-937.

Sha, W. Y., 2000. Advances in ocean tide research in China Sea. *Marine Forecasts*, **17** (2): 73-77 (in Chinese).

Shen, Y. J., and Ye, A. L., 1984. Numerical calculation of three-dimensional semidiurnal tidal flow field in the East China Sea. *Transactions of Oceanology and Limnology*, **1**: 1-10 (in Chinese with English abstract).

Teague, W. J., Perkins, H. T., Hallock, Z. R., and Jacobs, G. A., 1998. Current and tide observations in the southern Yellow Sea. *Journal of Geophysical Research*, **103**: 27783-27793.

Wan, Z. W., Qiao, F. L., and Yuan, L. Y., 1998. Numerical simulation of three-dimensional tidal current in the Bohai Sea, the Yellow Sea and the East China Sea. *Oceanologia et Limnologia Sinica*, **29** (6): 611-616 (in Chinese with English abstract).

Wang, K., Fang, G. H., and Feng, S. Z., 1999. A 3D numerical simulation of $M_2$ tides and tidal currents in the Bohai Sea, the Huanghai Sea and the East China Sea. *Acta Oceanologica Sinica*, **21** (4): 1-13 (in Chinese with English abstract).

Ye, A. L., 1984. Characteristic of the tidal current elliptic long axis direction variations with the rise of the depth. *Transactions of Oceanology and Limnology*, **2**: 1-6 (in Chinese with English abstract).

Ye, A. L., and Mei, L. M., 1995. Numerical simulation of tidal wave in the Bohai Sea. *Oceanologia et Limnologia Sinica*, **26** (1): 63-69 (in Chinese with English abstract).

Zhang, H., Zhu, J. R., and Wu, H., 2005. Numerical simulation of eight main tidal constituents in the East China Sea, Yellow Sea and Bohai Sea. *Journal of East China Normal University*, **3**: 71-77 (in Chinese with English abstract).

Zhao, B., Fang, G., Cao, D., et al. 1994, Numerical simulation of tide and tidal current in the Bohai Sea, the Yellow Sea and the East China Sea. *Acta Oceanologica Sinica*, **16** (5): 1-10 (in Chinese).

**(Edited by Xie Jun)**